International Journal of Thermophysics, Vol. 23, No. 4, July 2002 (© 2002)

Imaging of Thermal Conductivity with Sub-Micrometer Resolution Using Scanning Thermal Microscopy[1]

Y. Q. Gu,[2, 3] X. L. Ruan,[2] L. Han,[2] D. Z. Zhu,[2] and X. Y. Sun[2]

With the development of new emerging technologies, many objects in scientific research and engineering are of sub-micrometer and nanometer size, such as microelectronics, micro-electro-mechanical systems (MEMS), biomedicines, etc. Therefore, thermal conductivity measurements with sub-micrometer resolution are indispensable. This paper reports on the imaging of various micrometer and sub-micrometer size surface variations using a scanning thermal microscope (SThM). The thermal images show the contrasts indicating the differences of the local thermal conductivity in the sample. Thermal resistance circuits for the thermal tip temperature are developed to explain the heat transfer mechanism between the thermal tip and the sample and to explain the coupling between the local thermal conductivity and the topography in the test results.

KEY WORDS: microscale measurement; scanning thermal microscopy; temperature; thermal conductivity.

1. INTRODUCTION

The measurement of thermophysical parameters, such as temperature, heat flux, heat flow rate, thermal conductivity, etc., is important in science and engineering. Many kinds of measurement techniques have been developed to satisfy different needs in industry, science, and technology. However, the spatial resolution of all these techniques is above one micrometer. Scanning thermal microscopy has been proposed for measurements [1, 2] with a

[1] Paper presented at the Fourteenth Symposium on Thermophysical Properties, June 25–30, 2000, Boulder, Colorado, U.S.A.

[2] Department of Engineering Mechanics, Tsinghua University, Beijing 100084, People's Republic of China.

[3] To whom correspondence should be addressed. E-mail: gyp-dem@tsinghua.edu.cn

0195-928X/02/0700-1115/0 © 2002 Plenum Publishing Corporation

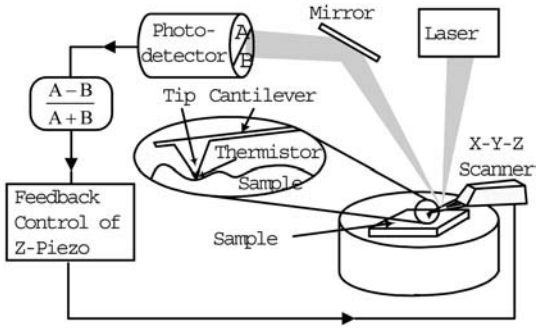

Fig. 1. Schematic of the scanning thermal microscope.

resolution of less than one micrometer. Although there have been many research papers on scanning thermal microscopy and a few scanning thermal microscope [SThM] products, the measurement mechanism is still not clearly understood. In this paper the measurement mechanism of SThM is analyzed using a thermal resistance circuit in its two operating modes, the temperature mode and the thermal conductivity mode. Al raster and silicon–silicon dioxide samples were tested using a commercially available scanning thermal microscope (Dimension 3100SPM, Digital Instrument Co.). The thermal images show the thermal conductivity contrast with sub-micrometer resolution, and the thermal images seem to be coupled with the topographical image in some manner.

2. MEASUREMENT PRINCIPLE

The scanning thermal microscope shown in Fig. 1 is based on the atomic force microscope (AFM), with a modified thermal probe to measure the temperature. The two ends of the probe are the base and the tip. Figure 2 shows the SEM image of the SThM tip with a pyramidal

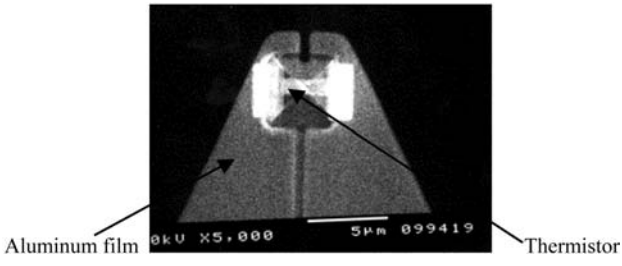

Fig. 2. SEM image of SThM probe tip.

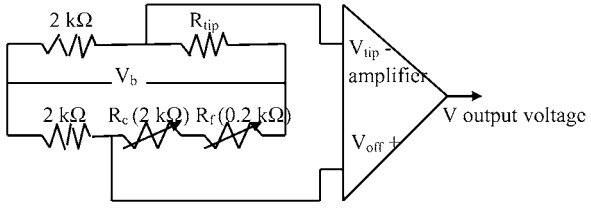

Fig. 3. Schematic of Wheatstone bridge circuit used in SThM.

shape and it has a thermistor deposited on it [3]. The thermistor changes resistance as a function of its temperature while being scanned across the sample. These changes are mapped relative to the tip's X- and Y-axis positions, resulting in a thermal image of the sample surface. The electronic circuit used to sense the temperature consists of a Wheatstone bridge and a differential amplifier as diagrammed in Fig. 3. The tip forms one of the legs of the Wheatstone bridge. Normally, a very small current passes through the probe to detect its resistance change, so its self-heating effect can be neglected. When the tip is at room temperature, offsets are adjusted so that $V = 0$. Then, as the tip heats up or cools down, the output signal V of the bridge is given as

$$V = k(T_t - T_0) \tag{1}$$

where T_t is the tip temperature, T_0 is the room temperature, and k is a constant that is a function of the amplifier gain, the electric bridge voltage, the thermistor's electrical resistance at room temperature and the temperature coefficient of resistance. The thermal image then represents the output V which is related to the tip temperature.

The scanning thermal microscope can operate in two modes: the temperature mode used to measure temperature and the thermal conductivity mode used to measure thermal conductivity.

2.1. Temperature Mode

In the temperature mode, the sample surface is at a higher temperature than room temperature. When the probe contacts the sample surface and scans continuously across it, heat will flow from the sample to the thermal tip. An equivalent thermal resistance circuit for this mode is illustrated in Fig. 4. R_c is the thermal resistance between the probe base and the tip, which is mainly a function of the cantilever material and is considered constant in the experiments. R_t is the thermal resistance between the tip and the sample surface which consists of the following components: R_g, the

thermal resistance due to gas conduction; R_w, the thermal resistance through the water film between the tip and the sample surface; R_{ss}, the thermal resistance through solid–solid contact; R_{con}, the thermal convection resistance; and R_r, the thermal radiation resistance. T_b is the temperature of the probe base, approximately equal to the room temperature T_0, T_t is the tip temperature, and T_s is the sample surface temperature. The sample is modeled as a heat source and the thermal capacity of the tip is very small; thus, the tip has little influence on the surface temperature during scanning.

When the tip contacts the sample surface, its curvature radius is about 50 nm. To simplify the computation, the contact length was estimated to be on a scale of 100 nm. The thermal resistance due to gas conduction R_g was estimated to be about 10^9 K·W^{-1}, the resistance through the water film was estimated to be about 10^5 K·W^{-1}, the solid–solid thermal resistance R_{ss} was estimated to be more than 10^7 K·W^{-1}, and R_{con} was estimated to be very large because the tip size is so small that convection between the tip and the sample is negligible [4]. When $T_t = 20°C$ and $T_s = 60°C$, the thermal resistance due to radiation R_r was estimated as [5]

$$R_r = \frac{(T_s - T_t)}{Q_r} = \frac{(T_s - T_t)}{C_0 F_1 \dfrac{(T_s^4 - T_t^4)}{100^4}} \approx 10^{10}\ \mathrm{K \cdot W^{-1}} \tag{2}$$

where C_0 is a radiation const, F_1 is the thermistor area and the view factor is equal to 1. If the view factor is less than 1, R_r will be larger.

Therefore, R_g, R_{con}, and R_r are large enough to be ignored since they are in parallel to R_w and R_{ss} which are much smaller. R_t is then given as

$$R_t = \frac{1}{\dfrac{1}{R_w} + \dfrac{1}{R_{ss}}} \tag{3}$$

R_w and R_{ss} are both related to the contact area between the tip and the sample. At high spots in the sample, the contact area is smaller, so R_w and R_{ss} are both larger, and R_t is larger, so R_t is related to the topography. Finally, the tip temperature is related to the sample surface temperature by

$$T_t = \frac{R_c}{R_c + R_t} T_s + \frac{R_t}{R_c + R_t} T_b \tag{4}$$

The output V is given by

$$V = k(T_t - T_b) = k(T_t - T_0) = k \frac{R_c}{R_c + R_t} (T_s - T_0) \tag{5}$$

Therefore, V is a function of T_s and R_t. Since R_t is related to the topography, V is also related to the topography, which means that the thermal image is coupled to the topographic image in the temperature mode.

Although it may prove difficult to precisely determine the local temperature, thermal imaging will give excellent contrast between sites having minor temperature differences.

2.2. Thermal Conductivity Mode

In the thermal conductivity mode, the probe base is radiated by a laser beam, while the measured sample is not heated, so the thermal tip temperature is higher than the sample temperature and heat flows from the tip to the sample. The thermal tip acts as both a detector and a heat source due to the laser beam irradiation. A 10 mW laser was used to illuminate the probe base. The equivalent thermal resistance network model is illustrated in Fig. 5.

In Fig. 5, T_b is the temperature of the illuminated area of the probe, R_c is the resistance between the laser spot and the tip, and R_λ is the internal resistance of the sample which is defined as $(T_s - T_0)/Q$. The sample temperature far from the tip can be considered to be uniform at the room temperature T_0. The tip temperature is given as Eq. (6) by the resistance network

$$T_t = \frac{R_c}{R_c + R_t + R_\lambda} T_0 + \frac{R_\lambda + R_t}{R_c + R_t + R_\lambda} T_b \tag{6}$$

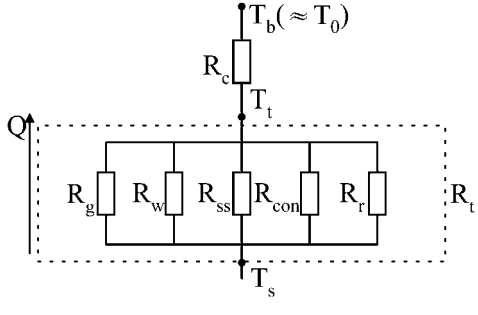

Fig. 4. Thermal resistance network for the temperature mode.

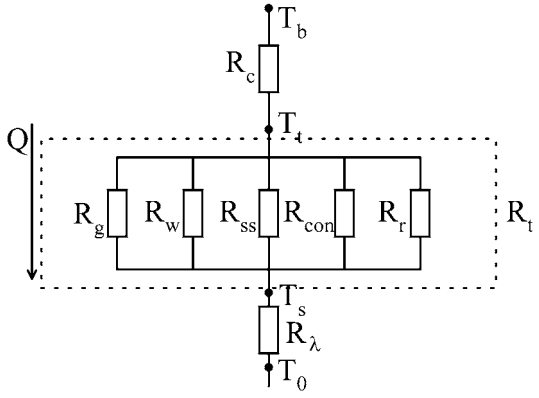

Fig. 5. Thermal resistance network for the thermal conductivity mode.

Then

$$T_t - T_0 = \frac{R_\lambda + R_t}{R_c + R_t + R_\lambda}(T_b - T_0) = Q(R_\lambda + R_t) \tag{7}$$

Because the laser power input into the cantilever is constant, so the heat flux Q is also constant. The output V is then related to R_t and R_λ as

$$V = k(T_t - T_0) = kQ(R_\lambda + R_t) \tag{8}$$

R_t varies in the scanning process and the internal resistance R_λ also varies with the scanning position if the material is inhomogeneous.

The tip is a moving heat source with a velocity of u relative to the sample as shown in Fig. 6. When the temperature distribution is quasi-stable, the moving heat source method can be used to calculate the excess temperature [6].

$$T_s - T_0 = \int_{-r_0}^{r_0} \int_{-\sqrt{r_0^2 - x^2}}^{\sqrt{r_0^2 - x^2}} \frac{1}{2\pi\lambda\sqrt{x^2 + y^2}} \frac{Q}{\pi r_0^2} e^{-\frac{u}{2a}(\sqrt{x^2+y^2}+x)} \, dy \, dx \tag{9}$$

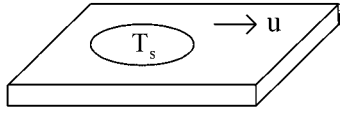

Fig. 6. The model of the heat transfer in the sample.

where the circular heat source is considered to be composed of many point heat sources, and r_0 is the heat source radius, a is the thermal diffusivity, and $r = \sqrt{x^2+y^2+z^2}$ is the distance from each point in the circle to the center of the circle.

So,

$$R_\lambda = \frac{T_s - T_0}{Q} = \frac{1}{2\pi^2 \lambda r_0^2} \int_{-r_0}^{r_0} \int_{-\sqrt{r_0^2-x^2}}^{\sqrt{r_0^2-x^2}} \frac{1}{\sqrt{x^2+y^2}} e^{-\frac{u}{2a}(\sqrt{x^2+y^2}+x)}\, dy\, dx \tag{10}$$

Actually, u, x, and y are very small during the scanning, so $e^{-\frac{u}{2a}(\sqrt{x^2+y^2}+x)} \approx 1 - \frac{u}{2a}(\sqrt{x^2+y^2}+x) \approx 1$ and then,

$$R_\lambda = \frac{T_s - T_0}{Q} = \frac{1}{\pi r_0 \lambda} = \frac{c}{\lambda} \tag{11}$$

Combining Eqs. (8) and (11) gives

$$V = kQ(R_\lambda + R_t) = kQ\left(\frac{1}{\pi r_0 \lambda} + R_t\right) \tag{12}$$

When R_t is constant, V will be smaller when λ is larger, so the thermal image reflects the thermal conductivity difference with the darker area responding to the higher thermal conductivity. Since R_λ is a function of λ and R_t is related the topography, then the signal V reflects the collective effect of the thermal conductivity and the topography. If λ is constant, but the topography is nonuniform, V will vary with the topography. Therefore, the thermal image is coupled to the topographic image in the thermal conductivity mode.

3. TESTS IN THERMAL CONDUCTIVITY MODE

3.1. Coupling of the Topographic and Thermal Images

Experiments on a one-dimensional Al raster with a line width of 666 nm were used to study the coupling of the topography and the thermal image. The raster material was uniform so the conductivity was uniform over the surface. Figure 7 shows the topographic image on the left and the thermal image on the right obtained simultaneously as the tip scanned across the sample. The bright regions in the thermal image, i.e., the higher temperature areas, correspond to the bright areas in the topographic image which were higher, even though there was no thermal conductivity difference in

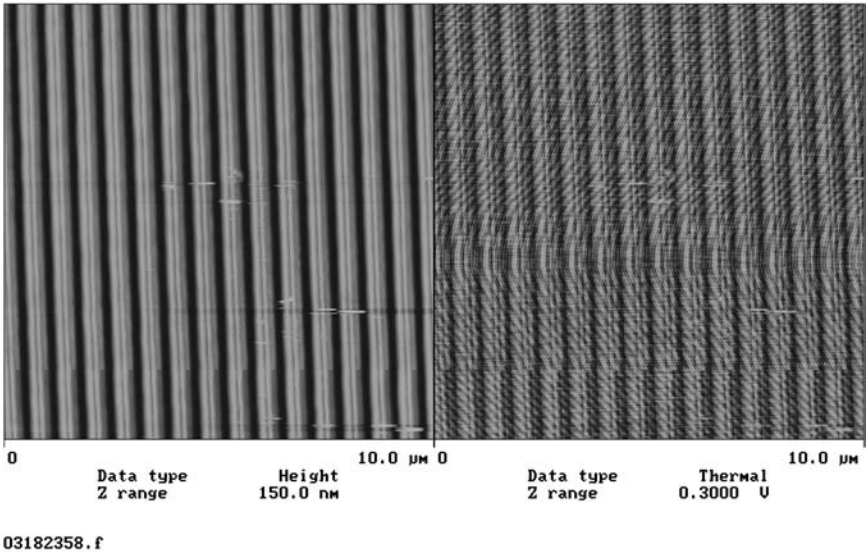

Fig. 7. Topographic (left) and thermal (right) image of Al raster (10×10 μm).

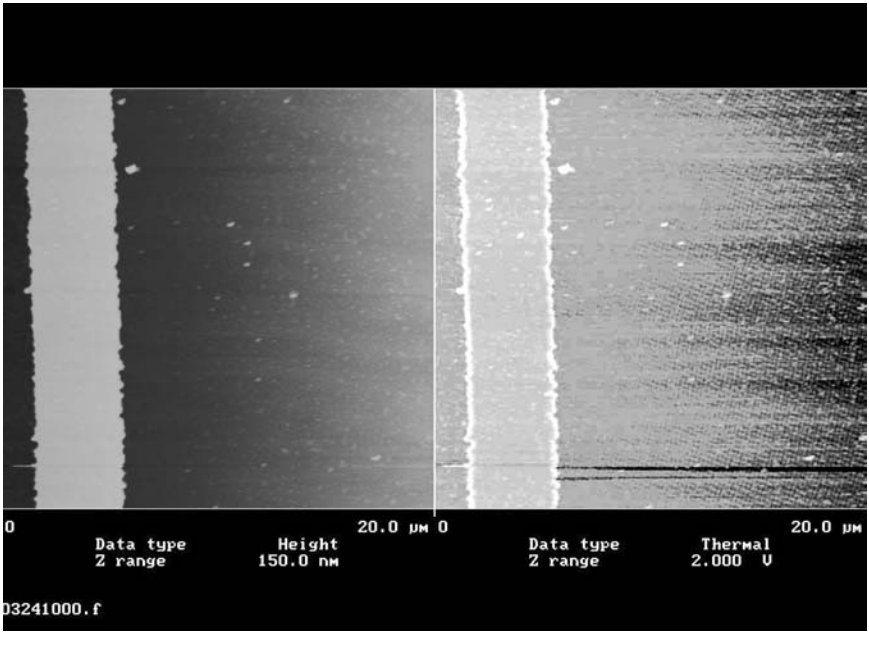

Fig. 8. Topographic (left) and thermal (right) image of SiO_2-Si sample (20×20 μm).

the sample at room temperature. The variations, therefore, illustrate the dependence of R_t on the topography.

3.2. Thermal Conductivity Contrast

Another experiment was done to illustrate the thermal conductivity contrast. Figure 8 shows the topographic and thermal images of a SiO_2-Si sample. The bright line in the topographic image is silicon dioxide, whereas the remainder is silicon. The topographic image shows that the SiO_2 region is 150 nm higher than the Si region. The silicon thermal conductivity is about one order of magnitude larger than that of silicon dioxide, so the tip temperature is lower when scanning across the silicon than when across the silicon dioxide. As a result, the Si region is darker in the thermal image.

Effective quantitative thermal conductivity measurements with SThM must consider the coupling effect due to the dependence of thermal resistance R_t on the topography. If a sample is composed of two different materials, A and B, then the ratio of their output V can be derived from Eq. (12):

$$\frac{V_A}{V_B}=\frac{(T_t-T_0)_A}{(T_t-T_0)_B}=\frac{R_{tA}+c/\lambda_A}{R_{tB}+c/\lambda_B}=\frac{\lambda_B}{\lambda_A}\cdot\frac{\dfrac{R_{tA}/R_{tB}}{\lambda_B/\lambda_A}+\dfrac{c}{\lambda_B R_{tB}}}{1+\dfrac{c}{\lambda_B R_{tB}}} \tag{13}$$

Therefore, the ratio of the outputs, V_A/V_B, can be related to λ_B/λ_A.

The thermal image in Fig. 8 was analyzed to obtain the average output voltages over the selected areas A for SiO_2 and B for Si shown in Fig. 9. V_A/V_B, the excess temperature ratio of the area A (over 2450 pixels) relative to the area B (over 9870 pixels), is equal to 5.6. Apparently, the ratio does not depend only on the thermal conductivity difference, because λ_B/λ_A, the standard thermal conductivity ratio of Si to SiO_2, is about 10. By Eq. (13), the discrepancy illustrates $\frac{R_{tA}}{R_{tB}}<\frac{\lambda_B}{\lambda_A}$ in our experiment and the importance of the topographic coupling.

4. CONCLUSIONS

A Dimension 3100 Scanning Thermal Microscope having two operative modes, the temperature mode and the thermal conductivity mode, can be used to measure surface temperature and thermal conductivity distributions with sub-micrometer spatial resolution. Thermal resistance circuits are developed for the two modes to explain the heat transfer mechanism

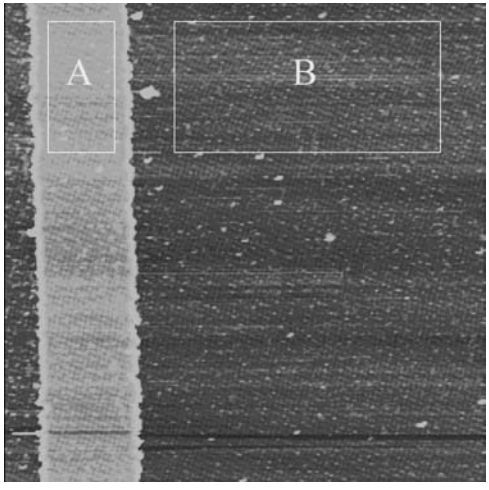

Fig. 9. Selected areas for estimation of tip temperature.

between the thermal tip and the sample surface. Thermal images were obtained in the thermal conductivity mode for a silicon wafer with a silicon dioxide line and for an Al raster sample. The microscale thermal images obtained in the thermal conductivity mode for inhomogeneous materials showed thermal conductivity coupling with the topography. The coupling was explained using the thermal resistance circuits.

ACKNOWNLEDGMENTS

This work is supported by the National Natural Science Foundation of China (No: 59776031 and 59995550-1). The authors are grateful to Prof. Litian Liu of the Institute of Microelectronics of Tsinghua University and Dr. Xiumei Wen of the Department of Engineering Mechanics of Tsinghua University for providing the samples.

REFERENCES

1. C. C. Williams and H. K. Wickramasinghe, *Appl. Phys. Lett*. **49**:1587 (1986).
2. A. Majumdar, *Experimental Heat Transfer* **9**:83 (1996).
3. Digital Instruments Corp., Support Note No. 235, Rev. A (1996).
4. K. Luo, Z. Shi, and J. Varesi, *J. Vacuum. Sci. Technol. B* **15**:349 (1997).
5. H. S. Jin, Y. Q. Gu, H. M. Chen, D. Z. Zhu, L. Han, and Z. G. Xie, *Acta Metrologica Sinica* **20**:266 (1999) (in Chinese).
6. E. R. G. Eckert and Robert M. Drake, Jr., *Analysis of Heat and Mass Transfer* (Hemisphere Publishing Corporation, 1987).